# The Negatively Acting Factors EID1 and SPA1 Have Distinct Functions in Phytochrome A-Specific Light Signaling[1]

**Yong-Chun Zhou, Monika Dieterle, Claudia Büche, and Thomas Kretsch***

Albert-Ludwigs-Universität Freiburg, Institut für Biologie 2/Botanik, Schänzlestrasse 1, D–79104 Freiburg, Germany

EID1 (empfindlicher im dunkelroten Licht) and SPA1 (suppressor of phytochrome A[phyA]-105) function as negatively acting components in phyA-specific light signaling. Mutants in the respective genes led to very similar phenotypes under weak-light conditions. To examine whether both genes are functionally redundant, detailed physiological and genetic analyses were performed with *eid1* and *spa1* mutants isolated from the same wild-type background. Measurements of hypocotyl elongation, anthocyanin accumulation, and *Lhcb1*-transcript accumulation under different light treatments demonstrated that SPA1 has a strong influence on the regulation of very low fluence responses and a weaker influence on high-irradiance responses. In contrast, EID1 severely altered high-irradiance responses and caused almost no change on very low fluence responses. Analyses on *eid1 phyA-105* double mutants demonstrated that EID1 could not suppress the phenotype of the weak *phyA* allele under continuous far-red light. Measurements on *eid1 spa1* double mutants exhibited a strong interference of both genes in the regulation of hypocotyl elongation. These results indicate that EID1 and SPA1 are involved in different but interacting phyA-dependent signal transduction chains.

Phytochromes are a family of plant photoreceptors that are adapted to sense red and far-red light. The functional photoreceptor molecules are dimers of approximately 125-kD subunits, whereby each monomer carries a phytochromobilin chromophore, a linear tetrapyrrole, covalently linked to a conserved Cys residue. The holoprotein is synthesized in its red-light-absorbing Pr form. Upon absorption of red light, the molecule can be photoconverted into the far-red-light-absorbing Pfr form. Similarly, the Pfr form can be photoconverted back into the Pr form when far-red light is absorbed. Because Pfr acts as a positive effector for physiological responses, phytochromes can function as photoreversible light switches when exposed to treatments with pulses of red and far-red light (Furuya and Schäfer, 1996; Whitelam and Devlin, 1997; Neff et al., 2000).

Phytochromes are encoded by a small multigene family in all plant species analyzed (Mathews and Sharrock, 1997). In Arabidopsis, five genes have been described named *PHYTOCHROME A* (*PHYA*) to *PHYE*. The gene products of *PHYB* to *PHYE* are light stable in Arabidopsis, whereby the *PHYB* gene shows the highest expression. The analyses of null mutants and overexpression studies demonstrated that light-stable phytochromes predominantly regulate light responses under continuous red and white light. They are also responsible for the so-called low fluence responses (LFR) that exhibit the classical red/far-red photoreversible characteristic of phytochrome function. LFR are normally induced by red-light photon fluences above approximately 1 $\mu$mol $m^{-2}$ (Furuya and Schäfer, 1996; Whitelam and Devlin, 1997; Neff et al., 2000; Weller et al., 2001).

The product of the *PHYA* gene is light labile and accumulates to very high levels in the dark (Clough and Viestra, 1997). Studies using phyA mutants and plants overexpressing phyA indicate that this photoreceptor is responsible for the very low fluence responses (VLFR) and for the far-red-light-dependent high-irradiance responses (HIR; Furuya and Schäfer, 1996; Whitelam and Devlin, 1997; Neff et al., 2000; Weller et al., 2001). Both responses do not show the classical red/far-red photoreversibility. VLFR can be induced with extremely low-photon fluences between 0.001 and 1 $\mu$mol $m^{-2}$, and even far-red-light pulses are very often sufficient for induction. The extent of the HIR depends on the duration and the fluence rate of the irradiation, and even short intervening dark phases result in a breakdown of the responses. Thus, the HIR sensory system must be able to detect the amount of photons that reach the plant in a given time period. The action spectra of HIR show a maximum at approximately 720 nm, a wavelength that completely inhibits responses of the light-stable phytochromes (Mancinelli, 1994; Furuya

[1] This work was supported by the Deutsch Forschungsgemeinschaft (grants "Signatransduktionsmutanten der Photomorphogenese von *Arabidopsis thaliana*" to E. Schäfer and T.K.) and by the Graduiertenkolleg "Molekulare Mechanismen der pflanzlichen Entwicklung."

* Corresponding author; e-mail kretsch@uni-freiburg.de; fax 49–761–203–2612.

Article, publication date, and citation information can be found at www.plantphysiol.org/cgi/doi/10.1104/pp.010811.

and Schäfer, 1996; Neff et al., 2000; Dieterle et al., 2001).

Various screening strategies have been used to isolate Arabidopsis mutants, which exhibit alterations in light regulation (Hardtke and Deng, 2000; Neff et al., 2000). Until now, at least eight independent genetic loci have been identified that exhibit reduced phyA responses. The target genes for *fhy3* and *fin2* are not yet identified (Whitelam et al., 1993; Soh et al., 1998). So far, *FHY1*, *FAR1*, *FIN219*, *PAT1*, and *HFR1/REP1/RSF1* have been characterized at the molecular level (Hudson et al., 1999; Bolle et al., 2000; Fairchild et al., 2000; Hsieh et al., 2000; Soh et al., 2000; Spiegelman et al., 2000; Desnos et al., 2001). HFR1, REP1, and RSF1 are allelic and code for a basic helix-loop-helix transcription factor that can form heterodimers with PIF3, another basic helix-loop-helix transcription factor involved in phytochrome signal transduction (Ni et al., 1998; Fairchild et al., 2000). The heterodimer binds to promoter elements present in many light-regulated genes. Most probably, the heterodimer also interacts with the Pfr form of phyA, which might lead to an induction of gene expression (Fairchild et al., 2000). The biochemical function of FHY1, FAR1, FIN219, and PAT1 is not yet defined.

Detailed physiological and genetic analyses could dissect phyA signal transduction in at least two branches that correspond to VLFR and HIR signaling. Yanovsky et al. (1997) could demonstrate that the Columbia (Col) ecotype does not respond to very low-light fluences. They identified two quantitative trait loci, *vlf1* and *vlf2*, that are responsible for the expression of VLFR. In contrast, *fhy3* mutants only exhibited defects in HIR, whereas mutations in the *FHY1* gene resulted in alterations in VLFR and HIR (Cerdán et al., 1999; Yanovsky et al., 2000).

Compared with the large number of mutants with reduced phyA responses, only two mutants, *spa1* and *eid1*, showed enhanced phyA-specific light responses (Hoecker et al., 1998; Büche et al., 2000; Dieterle et al., 2001). Both mutants accumulate normal levels of phyA, and phyA degradation in the mutants was not altered. Genetic and physiological results indicate that the encoded proteins function as negatively acting components of phyA signaling. SPA1 contains WD40 repeats similar to COP1 and exhibits some weak homology with protein kinases (Hoecker et al., 1999). Detailed analysis by Parks et al. (2001) demonstrated that light-induced growth promotion by SPA1 counteracts phytochrome-mediated growth inhibition during de-etiolation. EID1 is an F-box protein. F-box proteins are components of so-called SCF (Skp1/Cdc53/F-box protein) complexes that function as ubiquitin ligases. Thus, EID1 most probably acts by targeting activated components of phyA-signaling pathway to ubiquitin-dependent proteolysis (Dieterle et al., 2001).

The described phenotypes of *spa1* and *eid1* mutants were very similar. They exhibited hypersensitivity in all analyzed HIR under continuous far-red light, and both showed an increased sensitivity under weak continuous red light (Hoecker et al., 1998; Büche et al., 2000). However, it remained unclear whether these factors are functionally redundant and whether they are involved in independent or identical signal transduction chains. In a screening for novel hypersensitive mutants in phyA-signaling, we could isolate several *eid1* and *spa1* alleles in a Wassilewskija (WS) wild-type background. Because these alleles were present in the same ecotype, they could be used to compare different light responses of both mutations very accurately. The results obtained for different *spa1* and *eid1* mutants clearly indicate that both factors are not functionally redundant and that they are involved in different but interacting phyA-dependent signal transduction chains.

## RESULTS

### Characterization of Mutant Lines

A far-red-light field with low fluence rates was used to screen for hypersensitive mutants in phyA-dependent light signaling. Under these light conditions, the wild type remained almost completely etiolated, whereas hypersensitive mutants should exhibit a clear photomorphogenic development with expanded cotyledons, an open hook, and a reduced hypocotyl elongation (Dieterle et al., 2001). In total, eight independent mutant lines were isolated after screening approximately 20,000 T-DNA and approximately 30,000 EMS lines obtained in a WS background and approximately 10,000 T-DNA lines in a Col background. By complementation analysis, three mutants were identified as novel alleles of *spa1* and five mutants as novel alleles of *eid1*. Thus, all isolated mutants could be assigned to known genes.

The isolation of *eid1* and the *spa1* alleles from WS enabled a direct comparison of the function of these two genes in the same wild-type background. The *spa1* allele used in this study carries an artificial UAA stop codon instead of a CAA triplet that encodes for $Gln_{131}$. The resulting SPA1 protein should be terminated at this position instead of reaching its full length of 1,029 amino acids. The phenotype of the *spa1* allele was compared with the phenotypes of the strong *eid1-3* and the weak *eid1-5* allele (Dieterle et al., 2001). The *eid1-3* allele carries an insertion of a single basepair that leads to a frame shift at the 3′ end of the open reading frame. In the *eid1-5* allele, a Trp codon was mutated to a stop codon. The resulting truncated EID1 protein should consist of 156 instead of 336 amino acids.

### Photoreversibility in *eid1* and *spa1* Mutants

A unique property of the phytochrome system is its photoreversibility. To test whether the mutations in *SPA1* and *EID1* lead to a change in photoreversibil-

ity, seedlings were treated with multiple hourly light pulses of strong red light, strong RG9 light (extreme far-red light; $\lambda_{max}$ = 760 nm), and strong red immediately followed by RG9 light. The hourly pulse treatments were repeated for 3 d after the induction of germination before hypocotyl lengths were measured. The red/RG9 pulse program was established to screen for mutants the exhibit a loss of photoreversibility (Kretsch et al., 2000).

The *eid1* mutants and the wild type did not respond to hourly far-red-light pulse treatments, whereas multiple red-light pulse treatments induced the strongest effects (Fig. 1). Seedlings treated with red/RG9 pulses showed a weak photoreversion, but they never reached the hypocotyl length of plants treated with RG9-light pulses alone.

With *spa1* seedlings, a weak inhibition of hypocotyl elongation was detected even with the RG9-light pulse treatments, but hourly red-light pulses remained more effective (Fig. 1). Interestingly, repetitive red/RG9-light pulse treatments induced the strongest effects leading to reduction in hypocotyl elongation even below the level obtained for seedlings irradiated with multiple red-light pulses.

### Fluence Rate Response Curves for the Regulation of Hypocotyl Elongation under Continuous Irradiation

To analyze light sensitivity under continuous irradiation with different wavelengths, fluence rate response curves for hypocotyl elongation were measured for WS wild type, *spa1*, *eid1-3*, and *eid1-5* (Fig. 2). The seedlings were irradiated at different fluence rates for 3 d after the induction of germination before hypocotyl lengths were determined.

Fluence rate response curves of the WS wild type exhibited a typical sigmoid shape for most of the analyzed wavelengths, except for 692- and 699-nm light (Fig. 2, D and E). At these wavelengths, saturating irradiation was not achieved. In red light (between 628 and 672 nm), seedlings reached a relative hypocotyl length of about 0.4 at saturating photon fluence rates. Far-red light (708–737 nm) showed strongest inhibition of hypocotyl elongation at saturating photon fluence rates with relative hypocotyl length of approximately 0.2.

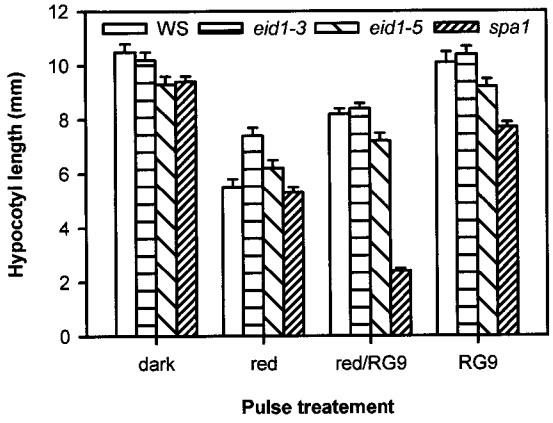


**Figure 1.** Analysis of hypocotyl elongation after treatments with hourly light pulses. Seedlings were either kept in darkness or were treated with hourly light pulses of red (30 s of 40 $\mu$mol $m^{-1}$ $s^{-1}$) or RG9 light (extreme far-red; 3 min of 36 $\mu$mol $m^{-2}$ $s^{-1}$), or red-light pulses immediately followed by photoreverting RG9-light pulses. Pulse treatments were administered for 3 d after the induction of germination. Error bars represent SE.

Compared with the WS wild type, the strong *eid1-3* and the weak *eid1-5* allele exhibited an increased light sensitivity at all wavelengths analyzed (Fig. 2). Hypocotyl length of *eid1* seedlings always reached the level of the dark controls or at least the levels observed for the wild type at very low-light fluence rates. In the red light (628–672 nm), both *eid1* alleles exhibited biphasic fluence rate response curves with an increase in relative hypocotyl length between approximately 0.1 and 0.01 $\mu$mol $m^{-2}$ $s^{-1}$ (Fig. 2, A–C). As demonstrated in a preliminary study, this local minimum in light sensitivity is caused by the onset of phyA degradation. Light effects below this fluence rates were clearly phyA dependent, whereas the responses at higher fluence rates could be attributed to phyB function (Büche et al., 2000). At wavelengths above 672 nm, fluence rate response curves exhibit a normal sigmoid shape (Fig. 2, D–I).

Seedlings of the *spa1* mutants always showed an increased light sensitivity when compared with the wild type (Fig. 2). The biggest difference between *spa1* and the other plants was seen at very low-light fluence rates. Whereas WS and *eid1* seedlings always reached the hypocotyl length of the respective dark controls in weak light, relative hypocotyl length of *spa1* seedlings did not increase above a level of approximately 0.7 to 0.8 (mean 0.72) even at the lowest photon fluence rates applied. Compared with *eid1*, *spa1* showed a higher sensitivity at very low fluence rates, but a lower sensitivity at intermediate or high fluence rates at wavelength below 737 nm. Thus, *spa1* seems be involved in a regulatory mechanism that can be saturated even with very low amounts of photons.

### Action Spectra for the Regulation of Hypocotyl Elongation

The fluence rate response curves in Figure 2 were used to calculate action spectra for hypocotyl elongation at wavelengths between 692 to 737 nm. Fluence rates leading to a relative hypocotyl length of 0.6 were determined using linear regression. To construct the action spectra, the value obtained for the wild type at 716 nm (0.166 $\mu$mol $m^{-2}$ $s^{-1}$) was set to 1 and the relative photon effectiveness for the wild type and the mutants at different wavelengths were calculated accordingly. For *spa1* a second, corrected action spectrum was calculated to eliminate possible errors caused by the differences in the shapes of its

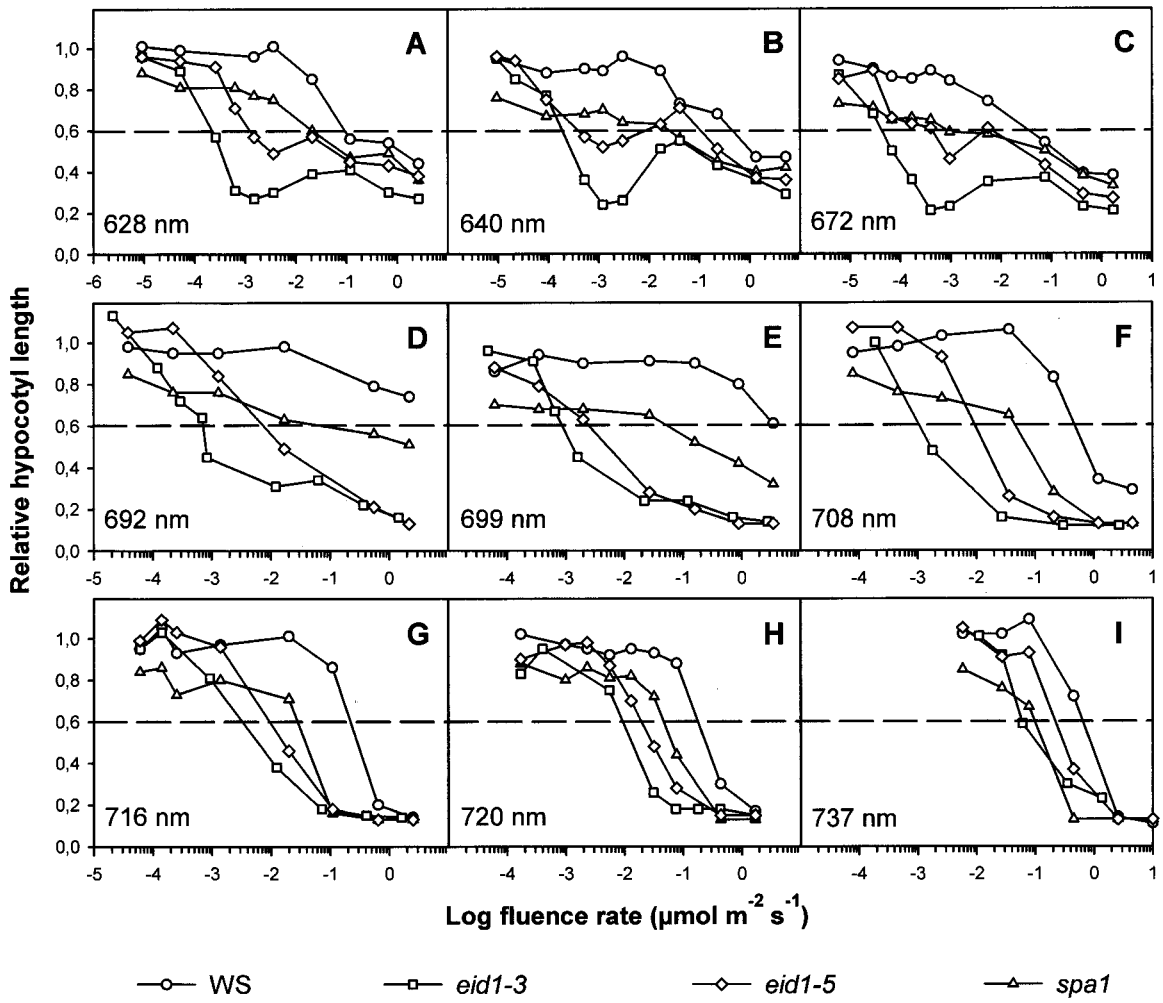


**Figure 2.** Fluence rate response curves for the inhibition of hypocotyl elongation under continuous light of different wavelengths. Hypocotyl lengths were measured 3 d after the induction of germination. The relative lengths were determined in relation to the length of dark-grown seedlings for each line. The hypocotyl lengths of dark controls correspond to those shown in Figure 1. SE of the individual measurements were between 0.05 and 0.1. Monochromatic light was obtained by interference filters. A, 628-nm DIL interference filter. B, 640-nm DIL interference filter. C, 672-nm DIL interference filter. D, 692-nm DEPIL interference filter. E, 699-nm DEPIL interference filter. F, 708-nm DEPIL interference filter. G, 716-nm DIL interference filter. H, 720-nm DEPIL interference filter. I, 737-nm DEPIL interference filter.

fluence rate response curves. To correct for the increased level of hypocotyl inhibition at the onset of the HIR in *spa1*, the mean of all values obtained for hypocotyl inhibition at the plateau level of the fluence rate response curves was determined. This mean (0.72) was set to 1 and fluence rate response curves were recalculated. Photon fluence rates that lead to a relative hypocotyl length of 0.6 were again determined as described above.

The wild type exhibited a typical HIR action spectrum with a maximum at 716 nm (Fig. 3A). The uncorrected and the corrected *spa1* action spectra exhibited an increase in light sensitivity compared with the wild type (Fig. 3B). Nevertheless, the overall shapes of the action spectra were very similar to the wild type and the maximum of the action spectra still remained at 716 nm.

The shape of the action spectra of the *eid1* alleles clearly differs from the action spectra of WS and *spa1* (Fig. 3C). Even though *eid1-3* and *eid1-5* revealed 50- and 17-fold higher relative photon effectiveness at 716 nm, their action spectra do not exhibit a typical HIR action spectrum with a maximum at 716 nm. Former analyses with *eid1 phyB* double mutants demonstrated that the respective action spectrum is very similar to the absorption spectrum of the Pr form of phytochromes (Dieterle et al., 2001).

### Inhibition of Hypocotyl Elongation under Multiple Far-Red-Light Pulse Treatments

A characteristic property of the HIR is its dependence on continuous irradiation. Even short, intervening dark phases normally lead to a loss of the

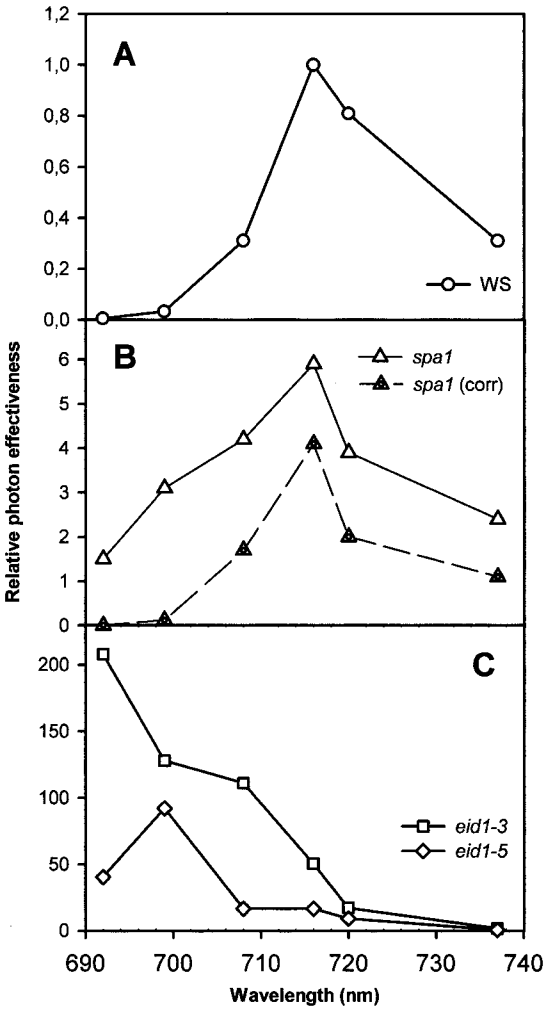


**Figure 3.** Action spectra for hypocotyl elongation. Fluence rate response curves shown in Figure 2 were used to determine the fluence rate that induced a relative hypocotyl length of 0.6. The value obtained for WS wild type at 720 nm (0.166 $\mu$mol $m^{-2}$ $s^{-1}$) was set to 1, and the relative photon effectiveness for the mutants and the wild type at different wavelength was calculated accordingly. A, Action spectrum for the WS wild type. B, Action spectra for *spa1*. The corrected action spectra [*spa1*(corr)] was determined to eliminate errors that might occur because of the different shape of the *spa1* fluence rate response curves (see Fig. 2). To correct for the increased level of hypocotyl inhibition at the onset of HIR in *spa1*, the mean of all values obtained for hypocotyl inhibition at the plateau level of the fluence rate response curves was determined. This mean (0.72) was set to 1, and fluence rate response curves were recalculated. Photon fluence rates that led to a relative hypocotyl length of 0.6 were again determined as described above. C, Action spectra for *eid1-3* and *eid1-5*.

response (Mancinelli, 1994; Büche et al., 2000). To study this effect, we administered repetitive far-red-light pulses (716-nm DAL interference filter light, 6 $\mu$mol $m^{-2}$ $s^{-1}$, 2.5 min) over 3 d after the induction of germination, whereby the duration of intermitting dark phases was varied. Hypocotyl length was measured at the end of the light treatments.

With WS wild type, even intermitting dark phases of 1 min resulted in a clear reduction in the response. WS seedlings reached a level for the relative hypocotyl length of about 0.9 at intermitting dark phases between 30 min and 2 h. The relative hypocotyl length of the dark control was reached when far-red-light pulses were given every 4 h (Fig. 4A).

The *spa1* mutant exhibited an increased persistence in the response toward multiple light treatments. The relative hypocotyl length increased up to an intermitting dark phase of 57 min and 30 s when it reached a plateau level similar to the results determined with fluence rate response curves. Even dark phases up to 4 h did not lead to a further decrease in the inhibition of hypocotyl elongation (Fig. 4A).

The weak *eid1-5* exhibited a clearly increased persistence toward multiple pulse treatments. Even intermitting dark-phases of up to 2 h were still effective (Fig. 4A). In contrast to *spa1* and similar to the WS wild type, *eid1-5* reached the level of its dark control when intermitting dark-phases were extended to 4 h. Comparable but much stronger effects were obtained for the *eid1-3* allele (Fig. 4A).

In principle, the light responses induced by multiple far-red pulse treatments can either be caused by signaling cascades inducing an HIR or a VLFR. Yanovsky et al. (1997) demonstrated that the Col ecotype is unable to respond to very low-light fluences. Therefore, experiments were performed with *eid1-6* and its respective Col wild type to test whether the increased persistence toward multiple far-red-light pulses in *eid1* can be suppressed by the loss of VLFR in this ecotype.

The Col and WS wild types exhibited very similar escape kinetics, even though WS seedlings always seemed to be more sensitive (Fig. 4B). Col seedlings reached the hypocotyl length of their dark controls when the intermitting dark phase is extended to 17 min and 30 s, whereas WS seedlings reached the level of the dark controls only with and intermitting dark phase of 4 h. This differences between Col and WS most probably reflect differences in the VLFR in both ecotypes. Nevertheless, *eid1-6* showed decay kinetic similar to *eid1-5*. Thus, the loss of VLFR in Col could not eliminate the increased persistence toward multiple far-red-light pulse treatments observed for hypocotyl elongation in *eid1*.

### Anthocyanin Accumulation under Multiple Far-Red-Light Pulse Treatments

Anthocyanin accumulation in Arabidopsis seedlings can be induced by a phyA-dependent HIR in far-red light, whereas hourly red-light pulses and continuous irradiation with strong red light did not result in an anthocyanin accumulation in WS, *spa1*, and *eid1-3* (data not shown). These results demonstrate that anthocyanin accumulation in the WS ecotype cannot be obtained under LF and VLF con-

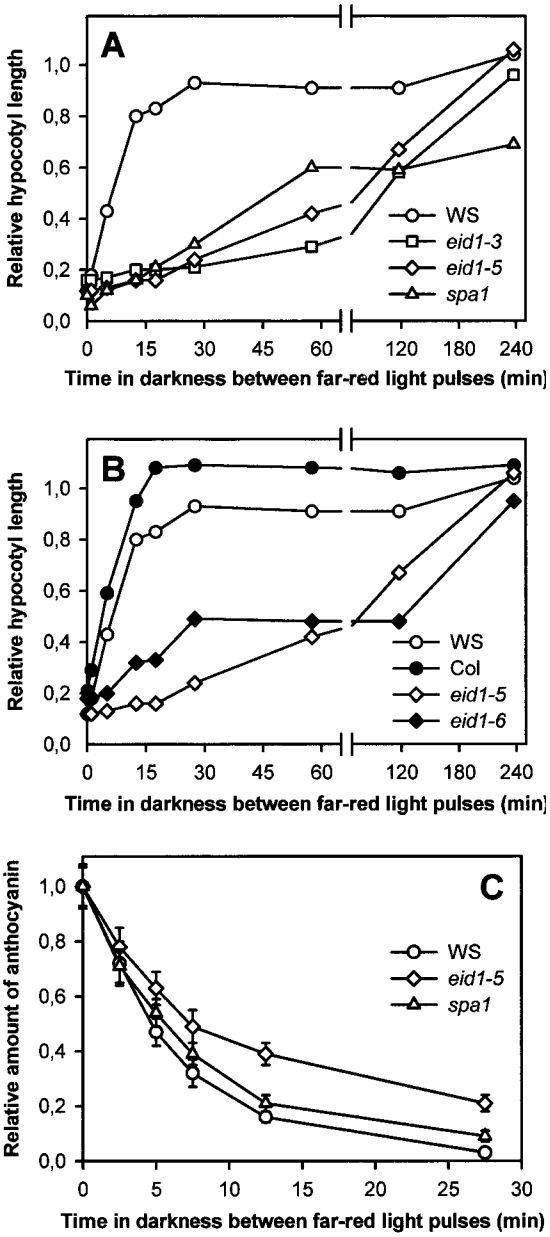


**Figure 4.** Hypocotyl elongation and anthocyanin accumulation under multiple far-red-light pulse treatments. Seedlings were irradiated with multiple far-red-light pulses (716-nm DAL interference filters) of 6 $\mu$mol $m^{-2}$ $s^{-1}$ for 2.5 min, varying the duration of the dark phases between the light pulses. Hypocotyl length and anthocyanin accumulation were determined after applying the pulse program for 3 d after the induction of germination. A, Relative hypocotyl length for WS, *spa1*, *eid1-3*, and *eid1-5*. The hypocotyl lengths of the dark controls correspond to those shown in Figure 1. B, Relative hypocotyl lengths for WS, Col, and *eid1-6*. Hypocotyl length of dark controls were 10.0 ± 0.2 mm for Col and 9.1 ± 0.2 mm for *eid1-6* (mean ± SE). C, Relative anthocyanin contents of WS, *spa1*, and *eid1-5* seedlings. Anthocyanin content was determined spectroscopically after extraction of 50 seedlings. The absolute absorption values obtained for continuous irradiation were 0.091 for WS, 0.094 for *spa1*, and 0.081 for *eid1-5*. Error bars represent SE.

ditions. Thus, measurements of anthocyanin accumulation would be an unambiguous proof to see whether an increased persistence toward multiple far-red-light pulses is caused by an alteration in the HIR decay kinetics.

Only a weak difference in the persistence of the HIR was obtained between *spa1* and the WS wild type. In contrast, a much stronger effect was detected with *eid1-5* (Fig. 4C). These results demonstrate that mutations in *EID1* can alter the decay kinetics of the HIR signaling cascade involved in anthocyanin accumulation.

### *Lhcb1* Transcript Accumulation under VLF and LF Conditions

Accumulation of *Lhcb1* transcripts shows a VLFR and a LFR in Arabidopsis (Cerdán et al., 2000). Furthermore, *Lhcb1* transcript accumulation can be induced by one single light pulse, which should eliminate problems that might occur upon multiple pulse treatments. Therefore, this response was chosen to analyze differences in VLFR and LFR between the two mutants and their WS wild type. Three-day-old etiolated seedlings were irradiated with single 1-min red-light pulses of various intensities and plants were harvested after an additional dark-incubation period of 4 h to allow maximum *Lhcb1* transcript accumulation.

In wild-type seedlings, *Lhcb1* transcript accumulation above the dark level was first detectable in the VLF range at photon fluences of about 0.01 to 0.1 $\mu$mol $m^{-2}$ (Fig. 5). A strong increase was also seen in the LF range at light fluences above 10 $\mu$mol $m^{-2}$.

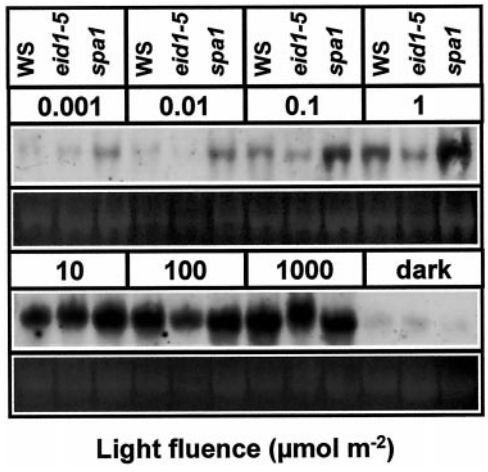


**Figure 5.** *Lhcb1* transcript accumulation under very low- and low fluence conditions. WS wild-type, *eid1-5*, and *spa1* seedlings were grown in darkness for 3 d after the induction of germination. Etiolated seedlings were treated with 1-min red-light pulses of variable photon fluence rates to obtain different light fluences. Plants were harvested 4 h after pulse treatment, and total RNA was isolated. *Lhcb1* transcript levels were measured by hybridization of the corresponding DNA probe to blots of 5 $\mu$g of total RNA. Fluorescent signals of 26S rRNA stained with ethidium bromide are shown as a loading control.

The onset of *Lhcb1* transcript accumulation in *eid1-5* seedlings was weakly shifted to higher light fluences in the VLF range, whereas the onset of LFR remained more or less unaltered (Fig. 5). Thus, mutations in the *EID1* gene seem to reduce the sensitivity of this VLFR.

Compared with wild type and *eid1-5*, *spa1* exhibited an extreme shift in light sensitivity under VLF conditions (Fig. 5). Light-dependent *Lhcb1* transcript accumulation was even detectable with the weakest red-light pulse applied (0.001 $\mu$mol $m^{-2}$). Compared with WS and *eid1-5*, *Lhcb1* transcript in *spa1* was clearly increased with light pulses of 0.01 to 10 $\mu$mol $m^{-2}$.

### Far-Red-Light Responses of the *phyA-105 eid1-3* Double Mutant

The *spa1* mutant was originally screened as a suppressor of the weak *phyA-105* allele under continuous far-red light (Hoecker et al., 1998). To test whether *eid1* can also suppress the *phyA-105* phenotype, *eid1 phyA-105* double mutants were isolated, and hypocotyl elongation was analyzed under continuous far-red light.

Both the Rschew (RLD) and the WS background lines exhibited similar fluence rate response curves, whereas the *eid1-3* mutant showed an increased light sensitivity (Fig. 6A). Neither the *phyA-105* mutant nor the *phyA-105 eid1-3* double mutant responded to continuous 725-nm light under the applied light fluence rates. Thus, *eid1-3* cannot suppress the *phyA-105* phenotype under the observed light conditions.

### Far-Red-Light Responses of the *eid1-5 spa1* Double Mutant

To test for an interaction of *eid1* and *spa1* function by genetic means, hypocotyl elongation of the single mutants and an *eid1-5 spa1* double mutant was analyzed under continuous far-red light (720-nm DIL filter). The *eid1-5 spa1* double mutant exhibited an extremely increased light sensitivity (Fig. 6B). The comparison of the fluence rate response curve of *eid1-5*, *spa1*, and *eid1-5 spa1* demonstrated that the light response in the double mutant is not simply additive. Reduction of hypocotyl elongation in *eid1-5 spa1* remained saturated at a fluence rate of 0.013 $\mu$mol $m^{-2}$ $s^{-1}$. Under the same fluence rate, *eid1-5* exhibited only a weak-light response and *spa1* reached its plateau level that remained unaltered even at much lower fluence rates. Furthermore, the double mutant showed an inhibition of hypocotyl elongation below the level of *spa1* even at 0.0056 and 0.0023 $\mu$mol $m^{-2}$ $s^{-1}$ that had nearly no effect with the *eid1-5* mutant. These results clearly indicated that EID1 and SPA1 do not function independently.

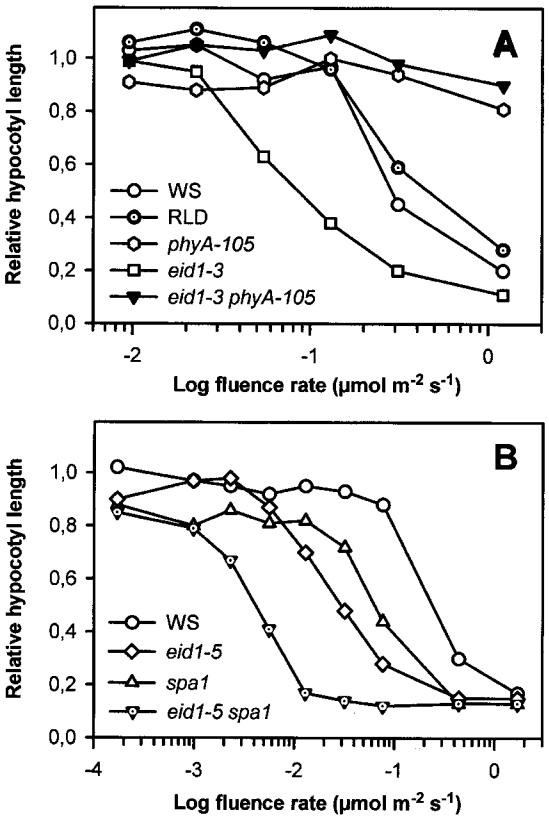


**Figure 6.** Fluence rate response curves for the inhibition of hypocotyl elongation for different wild types, single, and double mutants under continuous far-red light. Hypocotyl lengths were measured 3 d after the induction of germination. Relative lengths were calculated in relation to the length of the respective dark controls. Hypocotyl length of dark controls for WS, *eid1-3*, *eid1-5*, and *spa1* correspond to those shown in Figure 1. SE of individual measurements were between 0.05 and 0.1. Monochromatic light was obtained by interference filters. A, Fluence rate response curves for WS and RLD wild type, *eid1-3*, *phyA-105* (RLD background), and the *eid1-3 phyA-105* double mutant obtained with a 725-nm DEPIL interference filter. Hypocotyl length of dark controls were 9.2 ± 0.2 mm for RLD, 8.0 ± 0.3 mm for *phyA-105*, and 9.4 ± 0.2 mm for the double mutant (mean ± SE). B, Fluence rate response curves for WS wild type, *eid1-5*, *spa1*, and the *eid1-5 spa1* double mutant obtained with a 720-nm DEPIL interference filter. Hypocotyl length of dark controls were 7.8 ± 0.3 mm for the double mutant (mean ± SE).

## DISCUSSION

The data indicate that SPA1 functions as a negative factor in phyA-specific light signaling cascades regulating VLFR. Loss of SPA1 led to increased levels of *Lhcb1* transcripts under VLF conditions. An altered responsiveness in VLFR signaling also explains the observed hypersensitivity for the inhibition of hypocotyl elongation at extremely low-light fluence rates and upon multiple pulse treatments with far-red and extreme far-red (RG9) light. Furthermore, the loss of a negative regulator for VLFR might also be the reason for the observed hypersensitivity of *spa1* seedlings under multiple red/RG9 pulse treatments. Seedlings with increased VLFR would respond to both, red- and RG9-light pulses. The increased level of phyA under red/RG9 pulse treatments should further amplify this effect. Hourly short red-light

pulses normally induce a nearly complete degradation of phyA because of the formation of light labile Pfr, whereas photoreversion from Pfr back to Pr with RG9 light prevents complete proteolysis (data not shown).

In contrast to SPA1, EID1 seems not to be involved in the regulation of VLFR or has even a positive effect on the respective light responses. Fluence rate response curves for hypocotyl inhibition in *eid1* mutants always reach the level observed for the wild type at the lowest fluence rates applied. Mutations in *EID1* did not change the responsiveness to hourly RG9 pulse treatments and light sensitivity to multiple red/RG9, because Pfr levels adjusted by the extreme far-red-light pulses (Pfr/Ptot $<$ 1%; Beggs et al., 1981) remain to low to induce VLFR. Furthermore, *eid1* seedlings lost their ability to respond to multiple 716-nm light pulse treatments (Pfr/Ptot $\approx$ 5%; Beggs et al., 1981; Mancinelli, 1994) that can induce VLFR when the intermitting dark phase was increased to 4 h. Thus, *eid1* mutants behave like WS wild type under these light pulse treatments. Finally, *Lhcb1*-transcript accumulation is even reduced in *eid1-5* under VLF conditions.

SPA1 also alters the sensitivity of HIR (Hoecker et al., 1998; this paper), but its influence is only weak compared with the strong *eid1-3* and the weak *eid1-5* alleles. The different influences on HIR obtained for *spa1* and *eid1* became most obvious regarding the action spectra for hypocotyl elongation in far-red light. Mutations in *EID1* altered the spectral sensitivity completely and caused an extraordinary increase in sensitivity. The action spectra for *spa1* were very similar to the wild type and maximum sensitivity remained at 716 nm. The results of anthocyanin accumulation under multiple pulse treatments also exhibited only a rather weak influence of SPA1 on this HIR, whereas mutations in EID1 had a much stronger effect on this light response.

The observed differences between *eid1* and *spa1* cannot be attributed to differences in the strength of the alleles used for the experiments. The analyzed *spa1* allele carries a stop codon close to the N terminus of the protein that is localized in front of the strongest alleles analyzed by Hoecker et al. (1998, 1999). Furthermore, the two additional *spa1* alleles isolated in the WS background during our screenings exhibited the same alterations under all analyzed light conditions (data not shown). Finally, differences in the strength of the alleles cannot explain why the analyzed *spa1* allele has a stronger influence on VLFR but a reduced effect on HIR when compared with both *eid1* alleles. Thus, these observations clearly indicate that *eid1* and *spa1* have a distinct mode of action in phyA-specific light signaling. This interpretation is further underlined by the finding that even the strong *eid1-3* allele cannot suppress the weak *phyA-105* mutant, which carries an amino acid transition (Ala to Val) at position 893 of the apoprotein. The observed inability to suppress the *phyA-105* allele can also explain why Hoecker et al. (1998) could not isolate *eid1* mutants but five independent *spa1* alleles during their screening for extragenic suppressers of *phyA-105*.

Our data indicate that SPA1 mainly functions as a negative effector on VLFR, whereas EID1 is only involved in signaling cascades regulating HIR. With respect to their influence on VLFR and HIR, *spa1* and *eid1* resemble the loss-of-function mutants *fhy1* and *fhy3*, respectively. Mutations in the *FHY1* gene led to reduction in VLFR and HIR, whereas mutations in *FHY3* are mainly involved in HIR (Cerdán et al., 1999; Yanovsky et al., 2000). To explain their data with the *fhy* mutants, Yanovsky et al. (2000) proposed a model that assumes that FHY1 functions upstream of FHY3 because it is involved in both types of phyA-specific responses, VLFR and HIR. VLFR1, VLFR2, and FHY3 should function downstream of FHY1 in independent branches regulating VLFR or HIR. This model can be adapted to our findings by assuming that SPA1 functions together with FHY1 upstream of EID1 and FHY3 (Fig. 7A). This modified model would also explain why SPA1 is involved in VLFR and HIR signaling, why EID1 is unable to suppress the weak *phyA-105* allele, and why *spa1 eid1* double mutants exhibited a strong nonadditive interaction between both factors.

Nevertheless, this view on EID1 and SPA1 function is contradicted by the observed qualitative differences in *spa1* and *eid1* mutants with respect to HIR. If SPA1 functions upstream of EID1, *spa1* loss-of-function mutations should always lead to the same

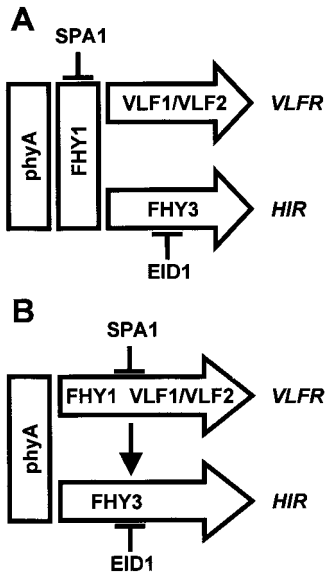


**Figure 7.** Proposed models for phyA signaling. Independent signaling cascades are given as large arrows. Lines indicate positive (→) or negative (⊣) interactions between the proposed independent signaling cascades. A, Model assuming that SPA1 function upstream of EID1. B, Model assuming that EID1 and SPA1 function on two branches divided early in phyA-specific light signaling.

changes in HIR as seen with *eid1* mutants. But *spa1* did not exhibit a biphasic shape of fluence rate response curves in red light, it did not change the HIR action spectra like *eid1*, and its influence on HIR was always lower when compared with *eid1*. This data indicate that branching in VLFR and HIR light signaling takes place very early in phyA-specific signal transduction. The differences between *spa1* and *eid1* mutants concerning the suppression of the *phyA-105* allele indicates that branching might even occur on the level of the photoreceptor molecule. According to our model, an EID1/FHY3-dependent pathway should be mainly involved in the regulation of the HIR under strong, continuous far-red light (Fig. 7B). This branch of phyA-dependent light signaling might have evolved to measure photon fluence rates, i.e. the amount of photons that reach the plant in a given time period (Büche et al., 2000). The SPA1/FHY1-dependent signaling cascade should be involved in the regulation of VLFR and other inductive phyA-dependent light responses, which depend on the photon fluence, i.e. the absolute amount of photons that reach the plant. The interaction between both branches of phyA light signaling should occur at later steps of the signaling cascades (Fig. 7B).

## MATERIALS AND METHODS

### Plant Material

For genetic crossing and physiological analyses, the following ecotypes and photomorphogenic mutants of Arabidopsis were used: Col, WS, RLD, *phyA-105* (ecotype RLD; Xu et al., 1995), *eid1-3*, *eid1-5*, *spa1* (all ecotype WS), and *eid1-6* (ecotype Col-7). All seeds were propagated in a phytochamber (Büche et al., 2000). The isolation of the mutants was described by Dieterle et al. (2001). Upon request, seeds of mutants will be made available in a timely manner for noncommercial research purposes. No restrictions or conditions will be placed on the use of any materials described in this paper that would limit their use in noncommercial research purposes.

### Isolation of Double Mutants

To isolate double mutant lines, the respective parental lines were crossed and $F_1$ plants were allowed to self-fertilize. Individual $F_2$ plants were analyzed by PCR-based markers to identify homozygous double mutants and approximately 20 seedlings of the $F_3$ generation were used to verify the result obtained for the $F_2$ plants. Seeds of the $F_3$ generation were used for further analyses. The *eid1-3* mutant (Dieterle et al., 2001) was crossed with *phyA-105* (Xu et al., 1995). *eid1-3 phyA-105* double mutants were identified by derived cleaved amplified polymorphic sequences marker analysis (Neff et al., 1998). For detection of the *phyA-105* mutation, PCR was performed using oligonucleotides 5′-ACTGGACAGGGAAGGTGTAGTGACAG-3′ and 5′-TACTTGACTTGTGGAAGCAGTCAACAC-3′. The PCR productwas analyzed for the presence (wild type) or absence of a *Tsp*RI restriction site (*phyA-105*). For the detection of the *eid1-3* mutation, a second PCR reaction was performed using oligonucleotides 5′-CTCGCTGTTT-GTTGTCCTGGTCTCTTCC-3′ and 5′-GTAAAGCAGTCC-AAGCACCAGAGACAGGAC-3′. The PCR product was digested with *Ava*II, which cuts the wild-type PCR product but not the *eid1-3* fragment. *eid1-5 spa1* double mutants were analyzed by cleaved amplified polymorphic sequences marker analysis (Konieczny and Ausubel, 1993). Genomic *EID1* fragments were amplified using the oligonucleotides 5′-CCGTGGAAGAAGAATGAAAGACCT-GTCCT-3′ together with 5′-CTCGCTGTTTGTTGTCCTG-GTCTCTTCC-3′. *Bsa*I could digest only DNA fragments obtained from eid1-5. To identify the *spa1* mutation, PCR was performed using the oligonucleotides 5′-AGTTTG-AGCATCTTTATCGTTTGGC-3′ together with 5′-GGC-CTCCTCCTATTCAAATCTTCGT-3′. Mutation in the *spa1* allele created an *Mbo*I restriction site that is absent in the wild-type allele.

### Seedling Growth and Light Sources

Seeds were sown on four layers of filter paper circles (595, Schleicher & Schüll, Dassel, Germany), which were placed in 94/16 petri dishes (Greiner, Kremsmünster, Austria) supplemented with 5 mL of distilled water. The standard sowing procedure was followed by 2 d of cold treatment at 8°C in the dark and 1 d of red-light induction of germination at 25°C before irradiation with different light treatments for 3 d. Induction of germination was performed with a standard light field (3.9 $\mu$mol $m^{-2}$ $s^{-1}$; Heim and Schäfer, 1982). For all other light treatments, modified Prado 500-W universal projectors (Leitz, Wetzlar, Germany) were used as light sources with Xenophot longlife lamps (Osram, Berlin). To measure fluence rate response curves, light was passed through narrow-banded DIL and DEPIL interference filters (Schott, Mainz, Germany). To analyze photoreversion, Arabidopsis seedlings were treated with a multiple pulse program of 30 s of red light (40 $\mu$mol $m^{-2}$ $s^{-1}$) followed by 5 min of extreme far-red light (36 $\mu$mol $m^{-2}$ $s^{-1}$) and 56 min and 30 s of darkness (Kretsch et al., 2000). Red light for all pulse treatments was obtained by passing the light beam through KG65 filters (Balzers, Liechtenstein, Germany). To get extreme far-red light, 8 mm-thick RG9 cut-off filters ($\lambda_{1/2}$ = 756 nm) were used (Schott). RG9 cut-off filters together with the Osram Xenophot longlife lamps resulted in a peak emission of the extreme far-red light at 760 nm. Far-red-light pulse treatments were performed with 716-nm DAL interference filters (Schott).

### Measurement of Hypocotyl Elongation and Anthocyanin Accumulation

Hypocotyl length was measured manually against a ruler. All data represent the mean of at least 40 seedlings analyzed in at least two independent experiments. Anthocyanin extraction and spectroscopic measurements were performed as described by Büche et al. (2000). All data

represent the mean of at least five independent experiments.

### Northern Analysis

After harvesting, samples were frozen immediately in liquid nitrogen and stored at −70°C. Total RNA was isolated with an RNeasy Plant Mini Kit (Qiagen, Hilden, Germany) using the RLC buffer for extraction. Northern blots were prepared according to standard procedures using 5 μg of total RNA and Duralon-UV membranes (Stratagene Europe, Amsterdam). A fragment of the Arabidopsis *Lhcb1-2* gene cloned into the pBluescriptsKS vector (Stratagene) was used as a probe. The probe was labeled with DIG-dUTP (Boehringer, Mannheim, Germany) by a PCR using the primers 5′-CGTCTAGATCAATGGCCGCCTCAACAATGGC-3′ and 5′-CGAATTCGCTCACTTTCCGGGAACAAAGTTGG-3′. Prehybridization, hybridization, washing, and detection were done as described in the manual of the DIG nucleic acid detection kit (Boehringer). The membrane was washed twice with 2× SSC/0.1% (w/v) SDS and twice with 0.1× SSC/0.1% (w/v) SDS at 68°C for 15 min.

## ACKNOWLEDGMENTS

We thank Martina Krenz for her excellent technical assistance throughout the project, Tim Kunkel for helpful discussions about the manuscript, Ute Hoecker and Peter Quail for the gift of *spa1* and *phyA-105* seeds, and Lars Hennig for the gift of the *Lhcb1* clone.

Received September 4, 2001; returned for revision October 23, 2001; accepted December 6, 2001.

## LITERATURE CITED

**Beggs CJ, Geile W, Holmes MG, Jabben M, Jose AM, Schäfer E** (1981) High irradiance response promotion of a subsequent light induction response in *Sinapis alba* L. Planta **151:** 135–140

**Bolle C, Koncz C, Chua N-H** (2000) PAT1, a new member of the GRAS family, is involved in phytochrome A signal transduction. Genes Dev **14:** 1269–1278

**Büche C, Poppe C, Schäfer E, Kretsch T** (2000) *eid1*: a new Arabidopsis mutant hypersensitive in phytochrome A-dependent high-irradiance responses. Plant Cell **12:** 547–558

**Cerdán PD, Staneloni RJ, Ortega J, Bunge MM, Rodriguez-Batiller MJ, Sánchez RA, Casal JJ** (2000) Sustained but not transient phytochrome A signaling targets a region of an *Lhcb1*2* promoter not necessary for phytochrome B action. Plant Cell **12:** 1203–1211

**Cerdán PD, Yanovsky MJ, Reymundo FC, Nagatani A, Staneloni RJ, Whitelam GC, Casal JJ** (1999) Regulation of phytochrome B by phytochrome A and FHY1 in *Arabidopsis thaliana*. Plant J **18:** 499–507

**Clough RC, Viestra RD** (1997) Phytochrome degradation. Plant Cell Environ **20:** 713–721

**Desnos T, Puente P, Whitelam GC, Harberd NP** (2001) FHY1: a phytochrome A-specific signal transducer. Genes Dev **15:** 2980–2990

**Dieterle M, Zhou Y-C, Schäfer E, Funk M, Kretsch T** (2001) EID1, an F-box protein involved in phytochrome A-specific light signaling. Genes Dev **15:** 939–944

**Fairchild CD, Schumaker MA, Quail PH** (2000) HFR1 encodes an atypical bHLH protein that acts in phytochrome A signal transduction. Genes Dev **14:** 2377–2391

**Furuya M, Schäfer E** (1996) Photoperception and signaling of induction reactions by different phytochromes. Trends Plant Sci **1:** 301–307

**Hardtke CS, Deng XW** (2000) The cell biology of the COP/DET/FUS proteins: regulating proteolysis in photomorphogenesis and beyond? Plant Physiol **124:** 1548–1557

**Heim B, Schäfer E** (1982) Light controlled inhibition of hypocotyl growth in *Sinapis alba* L. seedlings. Planta **154:** 150–155

**Hoecker U, Tepperman JM, Quail PH** (1999) SPA1, a WD-repeat protein specific to phytochrome A signal transduction. Science **284:** 496–499

**Hoecker U, Xu Y, Quail PH** (1998) SPA1: a new genetic locus involved in phytochrome A-specific signal transduction. Plant Cell **10:** 19–33

**Hsieh HL, Okamoto H, Wang M, Ang LH, Matsui M, Goodman H, Deng XW** (2000) FIN219, an auxin-regulated gene, defines a link between phytochrome A and the downstream regulator COP1 in light control of Arabidopsis development. Genes Dev **14:** 1958–1970

**Hudson M, Ringli C, Boylan MT, Quail PH** (1999) The FAR1 locus encodes a novel nuclear protein specific to phytochrome A signaling. Genes Dev **13:** 2017–2027

**Konieczny A, Ausubel FM** (1993) A procedure for mapping Arabidopsis mutations using co-dominant ecotype-specific PCR-based markers. Plant J **4:** 403–410

**Kretsch T, Poppe C, Schäfer E** (2000) A new type of mutation in the plant photoreceptor phytochrome B causes loss of photoreversibility and an extremely enhanced light sensitivity. Plant J **22:** 177–186

**Mancinelli AL** (1994) The physiology of phytochrome action. *In* RE Kendrick, GHM Kronenberg, eds Photomorphogenesis in Plants, Ed 2. Kluwer Academic Publishers, Dordrecht, The Netherlands, pp 51–59

**Mathews S, Sharrock RA** (1997) Phytochrome gene diversity. Plant Cell Environ **20:** 666–671

**Neff MM, Fankhauser C, Chory J** (2000) Light: an indicator of time and place. Genes Dev **14:** 257–271

**Neff MM, Neff JD, Chory J, Pepper AE** (1998) dCAPS, a simple technique for the genetic analysis of single nucleotide polymorphisms: experimental applications in *Arabidopsis thaliana* genetics. Plant J **14:** 387–392

**Ni M, Tepperman JM, Quail PH** (1998) PIF3, a phytochrome-interacting factor necessary for normal photoinduced signal transduction, is a novel basic helix-loop-helix protein. Cell **95:** 657–667

**Parks BM, Hoecker U, Spalding EP** (2001) Light-induced growth promotion by SPA1 counteracts phytochrome-mediated growth inhibition during de-etiolation. Plant Physiol **126:** 1291–1298

**Soh MS, Hong SS, Hanzawa H, Furuya M, Nam HG** (1998) Genetic identification of FIN2, a far-red light-specific signaling component of *Arabidopsis thaliana*. Plant J **16:** 411–419

**Soh MS, Kim YM, Han SJ, Song PS** (2000) REP1, a basic helix-loop-helix protein, is required for a branch pathway of phytochrome A signaling in Arabidopsis. Plant Cell **12:** 2061–2073

**Spiegelman JI, Mindrinos MN, Fankhauser C, Richards D, Lutes J, Chory J, Oefner PJ** (2000) Cloning of the Arabidopsis RSF1 gene by using a mapping strategy based on high-density DNA arrays and denaturing high-performance liquid chromatography. Plant Cell **12:** 2485–2498

**Xu Y, Parks BM, Short TW, Quail PH** (1995) Missense mutations define a restricted segment in the C-terminal domain of phytochrome A critical to its regulatory activity. Plant Cell **7:** 1433–1443

**Yanovsky MJ, Casal JJ, Luppi JP** (1997) The *VLF* loci, polymorphic between ecotypes Landsberg *erecta* and Columbia dissect two branches of phytochrome A signaling pathways that correspond to the very-low fluence and high-irradiance responses of phytochrome. Plant J **12:** 659–667

**Yanovsky MJ, Whitelam GC, Casal JJ** (2000) *fhy3-1* retains inductive responses of phytochrome A. Plant Physiol **123:** 235–242

**Weller JL, Perrotta G, Schreuder ME, van Tuinen A, Koornneef M, Giuliano G, Kendrick RE** (2001) Genetic dissection of blue-light sensing in tomato using mutants deficient in cryptochrome 1 and phytochromes A, B1 and B2. Plant J **25:** 427–440

**Whitelam GC, Devlin PF** (1997) Roles of different phytochromes in *Arabidopsis* development. Plant Cell Environ **20:** 752–758

**Whitelam GC, Johnson E, Peng J, Carol P, Anderson ML, Cowl JS, Harberd NP** (1993) Phytochrome A null mutants of Arabidopsis display a wild-type phenotype in white light. Plant Cell **5:** 757–768